



# $\beta$ -cells regeneration by WL15 of cysteine and glycine-rich protein 2 which reduces alloxan induced $\beta$ -cell dysfunction and oxidative stress through phosphoenolpyruvate carboxykinase and insulin pathway in zebrafish *in-vivo* larval model

Ajay Guru<sup>1</sup> · Gokul Sudhakaran<sup>1</sup> · Mikhlid H. Almutairi<sup>2</sup> · Bader O. Almutairi<sup>2</sup> · Annie Juliet<sup>3</sup> · Jesu Arockiaraj<sup>1</sup>

Received: 4 July 2022 / Accepted: 17 August 2022 / Published online: 12 October 2022  
© The Author(s), under exclusive licence to Springer Nature B.V. 2022, corrected publication 2023

## Abstract

**Background** Pancreatic  $\beta$ -cells are susceptible to oxidative stress, leading to  $\beta$ -cell death and dysfunction due to enhanced ROS levels and type 2 diabetes. To inhibit the  $\beta$ -cells damages induced by the oxidative stress, the present study investigates the beneficial effect of various peptides (WL15, RF13, RW20, IW13 and MF18) of immune related proteins (cysteine and glycine-rich protein 2, histone acetyltransferase, vacuolar protein sorting associated protein 26B, serine threonine-protein kinase and CxxC zinc finger protein, respectively). Also, the molecular mechanism of WL15 from cysteine and glycine-rich protein 2 on  $\beta$ -cell regeneration was identified through PEPCK and insulin pathway.

**Materials and methods** In this study, a total of five peptides including WL15, RF13, RW20, IW13, and MF18 were derived from immune-related proteins such as cysteine and glycine-rich protein 2, histone acetyltransferase, vacuolar protein sorting associated protein 26B, serine threonine-protein kinase and CxxC zinc finger protein, respectively. These protein sequences were obtained from an earlier constructed transcriptome database of a teleost *Channa striatus*. The identified peptides were evaluated for their antioxidant as well as antidiabetic activity. Based on the *in silico* analysis and *in-vitro* screening experiments, WL15 was predicted to have better antioxidant and antidiabetic activity among the five different peptides. Therefore, WL15 alone was further analyzed for apoptosis, antioxidant capacity, glucose metabolism, and gene expression performance, which was investigated on the alloxan (500  $\mu$ M) induced zebrafish *in vivo* larval model.

**Results** The results showed alloxan exposure to zebrafish larvae for a day, the ROS was generated in the  $\beta$ -cells. Interestingly, WL15 treatment showed a protective effect by reducing the toxicity of alloxan exposed zebrafish larvae by increasing their survival and heart rate. Moreover, WL15 reduced the intracellular ROS level and apoptosis in alloxan-induced larvae. The superoxide anion and lipid peroxidation levels are also reduced by improving the glutathione content after the WL15 treatment. Besides, WL15 treatment increased the proliferation rate of  $\beta$ -cells and decreased the glucose level. Further, the gene expression studies revealed that WL15 treatment normalized the PEPCK expression while upregulating the insulin expression in alloxan exposed larvae.

**Conclusion** Overall, the findings indicate that WL15 of cysteine and glycine-rich protein 2 can act as a potential antioxidant for type 2 diabetes patients in respect of improving  $\beta$ -cell regeneration.

**Keywords**  $\beta$ -cells · Cysteine and glycine-rich protein · Alloxan · PEPCK · Insulin pathway · Zebrafish

## Abbreviations

AGEs Advanced glycation end products  
PEPCK Phosphoenolpyruvate carboxykinase  
DHE Dihydroethidium  
NDA NDA, naphthalene-2,3-dicarboxal-dehyde

T2D Type 2 diabetes  
ROS Reactive oxygen species  
DCFDA 2'-7'-Dichlorofluorescein diacetate  
DPPP Diphenyl-1-pyrenylphosphine  
SD Standard deviation  
EDTA Ethylenediaminetetraacetic acid  
2-NBDG 2-[N-(7-nitrobenz-2-oxa-1,3-diazol-4-yl) amino]-2-deoxy-D-glucose  
DCFDA 2',7'-Dichlorodihydrofluorescein diacetate

✉ Jesu Arockiaraj  
jesuaraj@hotmail.com; jesuaroa@srmist.edu.in

Extended author information available on the last page of the article

CSRP2	Cysteine and glycine-rich protein 2
HATs	Histone acetyltransferase
VPS26B	Vacuolar protein sorting associated protein 26B
STPK	Serine threonine-protein kinase

## Introduction

The interplay between  $\beta$ -cell dysfunction and insulin resistance in the pathogenesis of diabetes is inherently complex [1]. When insulin-producing cells in pancreatic islets are unable to produce enough insulin to overcome peripheral insulin resistance, type 2 diabetes (T2D) develops, resulting in hyperglycemia. The  $\beta$ -cell dysfunction is linked to worsening glycemic control and treatment failure; it is critical to restoring  $\beta$ -cell functional mass in T2D management [2].  $\beta$ -cell mass is reduced in T2D patients due to increased apoptosis, oxidative stress, necrosis, and autophagy. In T2D, reactive oxygen species (ROS) are formed due to elevated glucose levels caused by  $\beta$ -cell dysfunction [3]. Increased ROS production in  $\beta$ -cells due to mitochondrial overstimulation inhibits the electron transport chain, resulting in lower energy production, DNA damage and the formation of advanced glycation end products (AGEs) [4]. The pancreatic  $\beta$ -cells with low antioxidant capacity are vulnerable to high endogenous production of ROS, implying that oxidative stress plays a major role in damaging the  $\beta$ -cells [5]. ROS such as superoxide and hydrogen peroxide are primarily produced during mitochondrial oxidative phosphorylation. Oxidative phosphorylation is tightly linked to insulin secretion in  $\beta$ -cells, where more than 90% of the carbons in glucose are oxidized to  $\text{CO}_2$  when the substrate supply is available [6]. The glucokinase in the  $\beta$ -cells has rate-limiting enzymes for glucose metabolism, which have a much lower affinity for glucose than other hexokinases, allowing the  $\beta$ -cell to control the rate of glucose metabolism. As a result, the rate of mitochondrial oxidation in the  $\beta$ -cell is directly proportional to blood glucose levels. It is widely accepted that when blood glucose levels are chronically elevated in T2D, increased oxidative phosphorylation leads to increased ROS production in  $\beta$ -cells [7].

The pancreas of zebrafish and humans are nearly identical, so larvae are widely used to study pancreatic toxicity. Alloxan can cause oxidative stress in  $\beta$ -cells of zebrafish larvae and is known to develop pancreatic cell dysfunction [8, 9]. Evidence based research has shown that peptide with antidiabetic and antioxidant activity plays a major role in treating T2D and its associated oxidative stress complications [10]. *Channa striatus* is a popular food fish in Southeast Asia. The pharmacological properties of this fish may have been influenced by its high concentrations of amino acids and fatty acids. Glycine, lysine and arginine are the

potent antioxidants present in this fish [11]. Antioxidant-rich foods have long been used to treat T2D by reducing oxidative stress and improving pancreatic cell proliferation and function. According to recent research, antioxidant molecules help to reduce hydrogen peroxide in  $\beta$ -cells to increase proliferation [12]. In this study, we aimed to screen the potential peptides identified from an earlier constructed transcriptome database (protein) of a teleost *C. striatus* and to evaluate the recovery effect of peptides on pancreatic  $\beta$ -cells toxicity through enhanced insulin expression and decreased transcriptional expression of phosphoenolpyruvate carboxykinase (PEPCK).

## Materials and methods

### *In-silico* studies.

#### Peptide rank and toxicity prediction

PeptideRanker (<http://distilldeep.ucd.ie/PeptideRanker/>) is a server that uses a novel N-to-1 neural network to predict bioactive peptides. The Peptide Ranker predicts whether a peptide sequence is likely to be bioactive by giving scores ranging from 0 to 1. A peptide score of more than 0.75 indicates that a sequence has the potential to be bioactive [13]. ToxinPred was used to calculate the toxicity of predicted T-cell epitopes (<http://crdd.osdd.net/raghava/toxinpred/>). ToxinPred is a computer programme that predicts which peptides are toxic or non-toxic [14].

#### HPEPDOCK

HPEPDOCK (<http://huanglab.phys.hust.edu.cn/hpepdock/>) is a server that uses a hierarchical algorithm to investigate protein-peptide docking. The results obtained from the protein–ligand binding affinity are expressed in kcal/mol units of free energy. In the discovery studio software (Version 4.1), the interaction between the peptide and the receptor is visualized [15, 16].

### *In-vitro* analysis.

#### $\alpha$ -amylase inhibition

To perform the  $\alpha$ -amylase inhibition assay, the solution was prepared with 0.01 M  $\text{CaCl}_2$  and 0.5 M Tris–HCL (pH 6.9) added to 2 mg of starch. This mixture was kept in a boiling water bath for 5 min. The various concentrations (10  $\mu\text{M}$  to 50  $\mu\text{M}$ ) of peptides (WL15, RF13, RW20, IW13, and MF18) were added to the reaction mixture and further added with pancreatic amylase dissolved in Tris–HCL buffer. The centrifugation was done to obtain the supernatant at 4000 rpm

for 10 min. This resultant supernatant was measured at 595 nm in a spectrophotometer (UV 1800, SHIMADZU, Kyoto, Japan) [17].

### Hydroxyl radical scavenging assay

To identify antioxidant activity, hydroxyl radical scavenging assay was performed [18]. The peptides with different concentrations were added to the reaction mixture containing EDTA (6 mM), ferrous sulphate (2 mM), PBS (0.2 mM), and phenanthroline (2 mM). Finally, 40  $\mu$ L of 0.03%  $H_2O_2$  was added to the reaction mixture and kept for 30 min incubation at 37 °C. Using a spectrophotometer, the absorbance was measured at 536 nm.

### Experimental zebrafish larvae.

The wild-type zebrafish of AB strain were purchased from the NSK Aquarium at Kolathur, Tamil Nadu, India. To obtain embryos, a spawning tank was maintained with male and female fish in a 2:1 ratio, and a mesh was kept at the bottom of the tank to prevent fish from eating its eggs. At the start of the light cycle, spawning took place. After 2 h of spawning, the embryos are collected and incubated in a 12 well plate with an embryo medium at 28 °C [19, 20, 21]. The larvae were incubated with 500  $\mu$ M alloxan for 1 day to induce oxidative stress in  $\beta$ -cells of larvae. For  $\beta$ -cells damage, the larvae were exposed to 500  $\mu$ M alloxan for 3 days. The larvae were divided based on the treatment groups (n = 100 each). The control group, in which larvae were untreated; whereas, in alloxan group, the larvae were exposed to 500  $\mu$ M alloxan; and the WL15 peptide treated group, the larvae were treated with different concentrations of WL15. All of the experiments were done per the Institute's Animal Ethical Clearance guidelines (No. SAF/IAEC/211215/004).

### Toxicity analysis in larvae

The protective effect of the WL15 peptide in alloxan-induced toxicity was investigated in 72 hpf zebrafish larvae [22, 23]. Briefly, different concentrations of the WL15 peptide were cotreated with alloxan and incubated for 24 h. The protective effect of WL15 was determined after the incubation period by calculating the mortality rate, heart rate, and percentage of deformities.

### Measurement of alloxan mediated stress

The ROS, apoptosis, and lipid peroxidation level were measured using the 2'-7'-dichlorofluorescein diacetate (DCFDA), Diphenyl-1-pyrenylphosphine (DPPP) and acridine orange staining [24, 25, 26]. In brief, the larvae were exposed

to 500  $\mu$ M of alloxan for 1 day and cotreated with WL15 (50  $\mu$ M). After treatment, the larvae were incubated for 1 h at room temperature in the dark with fluorescent stain (20  $\mu$ g/mL). The larvae were washed and anesthetized with ice-cold PBS for visualization after incubation. The fluorescent microscope equipped with CoolSNAP-Pro colour digital camera (Olympus, Tokyo, Japan) was used to capture the larvae stained with fluorescent dye. The fluorescent intensity was measured using Image J software (Version 1.49, NIH, USA).

### Quantification of superoxide anion and glutathione

The intracellular superoxide anion and glutathione depletion levels were measured using a modified version of a previously described protocol [27]. The larvae were incubated in the dark at 28.5 °C for 30 min with 20  $\mu$ M of dihydroethidium (DHE) and naphthalene-2,3-dicarboxaldehyde (NDA). The larvae were washed in PBS buffer after incubation. Fluorescence microscopy was used to capture the images, and the intensity of fluorescent was measured using Image J software.

### 2NBDG uptake

The 2NBDG uptake assay in zebrafish larvae was performed as described previously [28]. The 72 hpf larvae were placed in a 6-well plate, exposed to 500  $\mu$ M of alloxan, and cotreated with WL15 (50  $\mu$ M) for 3 days. After treatment, the larvae were stained with 2NBDG and kept for 3 h of incubation. The stained larvae were washed with PBS buffer to remove the excess stain and anesthetized for visualization. A fluorescent microscope captured the image of 2NBDG uptake in  $\beta$ -cells of zebrafish larvae.

### Glucose estimation in larvae

The treated zebrafish larvae from each group are taken to estimate the glucose level as per the test kit instructions (Robonik, India). The larvae were homogenized with 200  $\mu$ L PBS buffer and centrifuged at 5000 g for 10 min. The supernatant obtained after the centrifugation process was used for analysis. The supernatant was added to the microplate reader to measure the glucose level at 510 nm.

### Measurement of insulin and PEPCK gene expression

Using TRIzol Reagent method [29], the total RNA was isolated from untreated larvae, alloxan-exposed larvae, and WL15 treated larvae. The 1  $\mu$ g of isolated RNA was converted into first-strand cDNA for real-time PCR using a cDNA reverse transcription kit. Amplification was performed in a cDNA mixture on a Light Cycler 96 Real-Time

PCR machine using SYBER Green PCR Master Mix, with a final reaction volume of 20  $\mu$ L. PCR was carried out using the primers listed in Table 3. The  $2^{-\Delta\Delta C_t}$  method was used to determine relative gene expression [30, 31].

### Statistical analysis

GraphPad Prism was used to perform the statistical analysis (version 5.0). All experiments were done in triplicate, and statistical significance was determined by a *p* value of less than 0.05. The data were presented as a mean and standard deviation (SD).

## Results

### In silico analysis.

The peptides including WL15 (<sup>1</sup>WHKNCFRCAKCGKSL<sup>15</sup>), RF13 (<sup>1</sup>RRGKGRRVTMSF<sup>13</sup>), RW20 (<sup>1</sup>RPVKRKKGWPKGVKRGPPKW<sup>20</sup>), IW13 (<sup>1</sup>IKHFKKQRRLLIPW<sup>13</sup>) and MF18 (<sup>1</sup>MRKKA VKV KHV KRRREKKF<sup>18</sup>) derived from the protein sequence of cysteine and glycine-rich protein 2 (CSR2P2), histone acetyltransferase (HATs), vacuolar protein sorting associated protein 26B (VPS26B), serine threonine-protein kinase (STPK), and CxxC zinc finger protein (CxxC), respectively of an earlier constructed transcriptome dataset (protein sequence) of an teleost *C. striatus* were evaluated for toxicity using ToxinPred. Results showed that all the peptides were non-toxic (Table 1). PeptideRanker was used to screen these non-toxic peptides for the possibility of highly bioactive peptides. The WL15 has the highest PeptideRanker score of 0.93, indicating that this peptide was highly bioactive (Table 2). In contrast, MF18 has the lowest Peptide Ranker score of 0.23, with the least bioactive peptide possibility.

The HPEPDOCK tool was used to study the peptides (WL15, RF13, RW20, IW13, and MF18) interaction with the insulin receptor and glutathione (E-Suppl. Fig. 1). The binding score of the peptides with receptors is given in Table 2. The maximum binding affinity was noticed in the WL15

**Table 1** Toxicity prediction of the peptide (WL15, cysteine and glycine rich protein 2; RF13, vacuolar protein sorting associated protein 26B; RW20, histone acetyltransferases; IW13, serine threonine protein

S. No	Peptide	Sequence	Net hydrogen	Hydrophilic nature	Hydrophobic nature	Charge	pI	Mol. wt. (Da.)
1	WL15	WHKNCFRCAKCGKSL	1.00	0.05	-0.29	4.50	9.52	1781.35
	RF13	RRGKGRRVTMSF	1.54	0.74	-0.51	5.00	12.48	1507.96
3	RW20	RPVKRKKGWPKGVKRGPPKW	1.30	0.86	-0.49	9.00	12.32	2386.23
4	IW13	IKHFKKQRRLLIPW	1.38	0.26	-0.39	5.50	12.03	1750.37
5	MF18	MRKKA VKV KHV KRRREKKF	1.56	1.32	-0.63	9.50	11.78	2297.16

**Table 2** Peptide analysis by Peptide Ranker and HPEPDOCK

Peptide	Peptide Ranker Score	HPEPDOCK Binding affinity	
		Insulin receptor (PDB ID: 1IR3)	Glutathione (PDB ID: 2I3Y)
WL15	0.93	-218.16	-200.74
RF13	0.36	-189.35	-184.87
RW20	0.855	-191.54	-199.05
IW13	0.67	-186.32	-198.49
MF18	0.23	-177.15	-177.04

peptide; its insulin receptors are -218.16 kcal/mol units, and its glutathione is -190.74 kcal/mol units compared to other peptides Table 3.

### *In-vitro* $\alpha$ -amylase inhibition assay.

The  $\alpha$ -amylase inhibition activity revealed that at a minimum concentration of 10  $\mu$ M, WL15 inhibited 15%, RF13 inhibited 5%, RW20 inhibited 13%, IW13 inhibited 5%, and MF18 inhibited 2%. At a higher concentration of 50  $\mu$ M, WL15 inhibited 62%, RF13 inhibited 30%, RW20 inhibited 51%, IW13 inhibited 23% and MF18 inhibited 15% compared to the control glimepiride (74%) (*p* > 0.05) at 50  $\mu$ M. The WL15 peptide exhibited better antidiabetic activity than other peptides (E-Suppl. Fig. 2) considered for analysis.

### *In-vitro* antioxidant activity.

The antioxidant activity of the WL15, RF13, RW20, IW13, and MF18 was preliminarily screened using hydroxyl radical scavenging activity. In this assay, at a minimum concentration of 5  $\mu$ M, WL15 inhibited 12%, RF13 inhibited 4%, RW20 inhibited 7%, IW13 inhibited 5%, and MF18 inhibited 3%. At a higher concentration of 50  $\mu$ M, WL15 inhibited 69%, RF13 inhibited 23%, RW20 inhibited 47%, IW13 inhibited 23% and MF18 inhibited 20% compared to the control Trolox (79%) (*p* > 0.05) at 50  $\mu$ M. These results showed that the WL15 peptide had a better free radical scavenging activity compared to other peptides (E-Suppl. Fig. 3).

kinase; MF18, CxxC zinc finger protein) by ToxinPred. The analysis predicted all the peptides are non-toxic

**Table 3** Primers used in the gene expression study

Genes	Forward primer sequence	Reverse primer sequence	Reference
PEPCK	5'- GTTTGTAGGGGCGTC CATGA-3'	5'-CGTGGAAGATTTTGGGCA GC-3'	[39]
Insulin	5'- TGGTCGTGTCCAGTGTA AGC-3'	5'-GAAGGGGCTCAACGTCTC TC-3'	[39]
$\beta$ -actin	5'-GCAGAAGGAGATCACATCCCTGGC-3'	5'-CATTGCCGTCACCTTCACCGTTC-3'	[39]

### Protective effect of WL15 in zebrafish larvae.

The mortality and heartbeat rate of alloxan induced zebrafish larvae was reduced when cotreated with different concentration (10  $\mu$ M, 20  $\mu$ M, 30  $\mu$ M, 40  $\mu$ M, and 50  $\mu$ M) of WL15 (E-Suppl. Fig. 4A and 4B). The analysis revealed that cotreatment of the WL15 prevented the morphological abnormalities caused by the alloxan (500  $\mu$ M) (E-Suppl. Fig. 5A and 5B). The larvae with no morphological

abnormalities were found in the WL15 cotreatment at 40  $\mu$ M and 50  $\mu$ M.

### Reduction of oxidative stress in $\beta$ -cells.

The effect of WL15 on reducing ROS, apoptosis, and lipid peroxidation generated by alloxan in  $\beta$ -cell of zebrafish larvae was stained using DCFDA, acridine orange, and DPPH staining. The increase in fluorescent intensity was observed in alloxan exposed larvae, indicating enhanced ROS (82%),

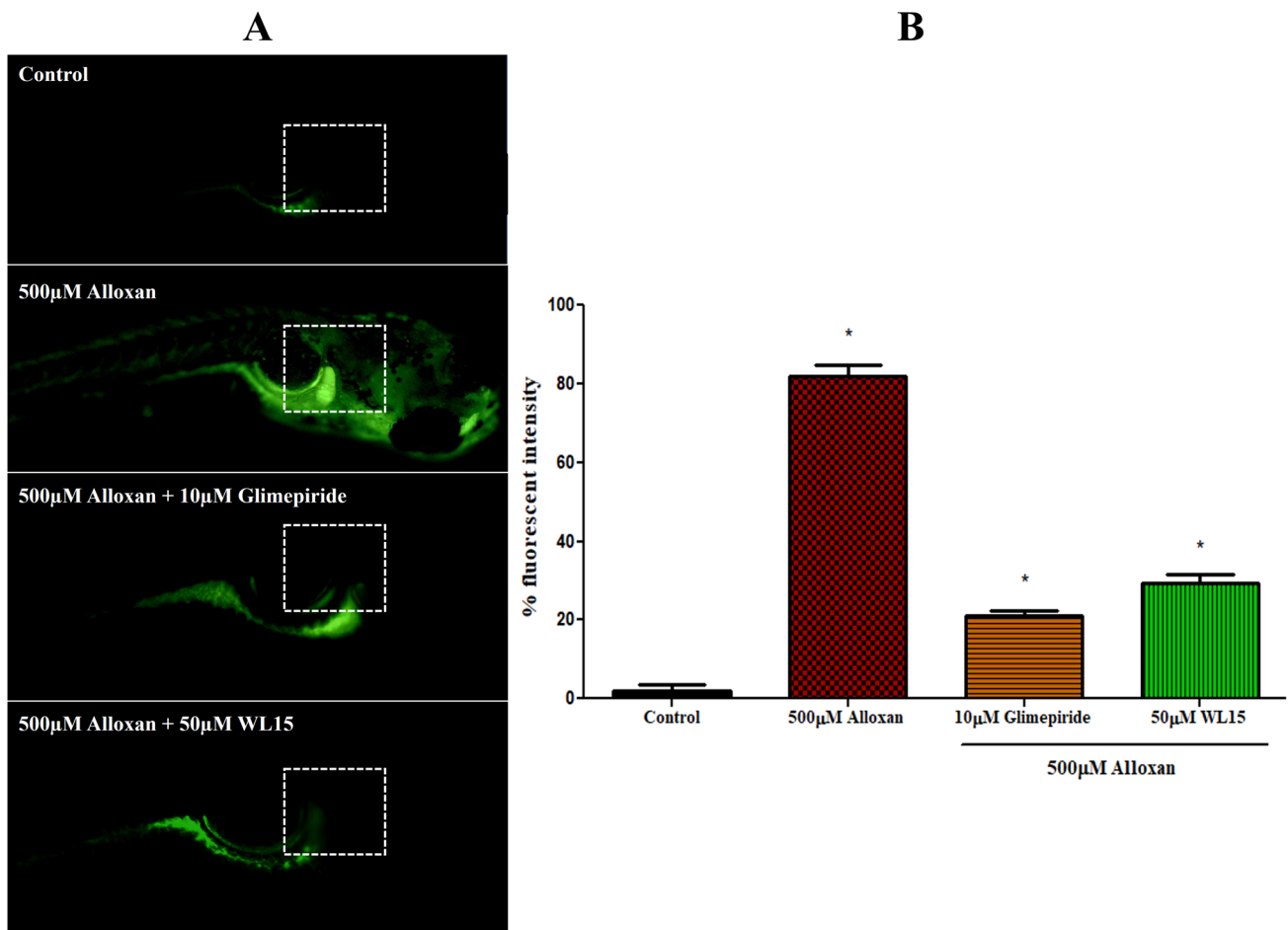


**Fig. 1** **A** Representative photomicrographs of oxidatively stressed  $\beta$ -cells in zebrafish larvae ( $n=10$ /group) stained by DCFDA fluorescent probe. **B** Quantitative analysis of *in-vivo* ROS generation in  $\beta$ -cells of zebrafish larvae. The fluorescence intensity was quantified using ImageJ. The untreated and glimepiride (10  $\mu$ M) larvae were

used as control and positive control in the experiment, respectively. The  $\beta$ -cells are marked inside the white box. Experiments were performed in triplicate, and the data were expressed as mean  $\pm$  SD. \* represents the statistical significance at  $p < 0.05$

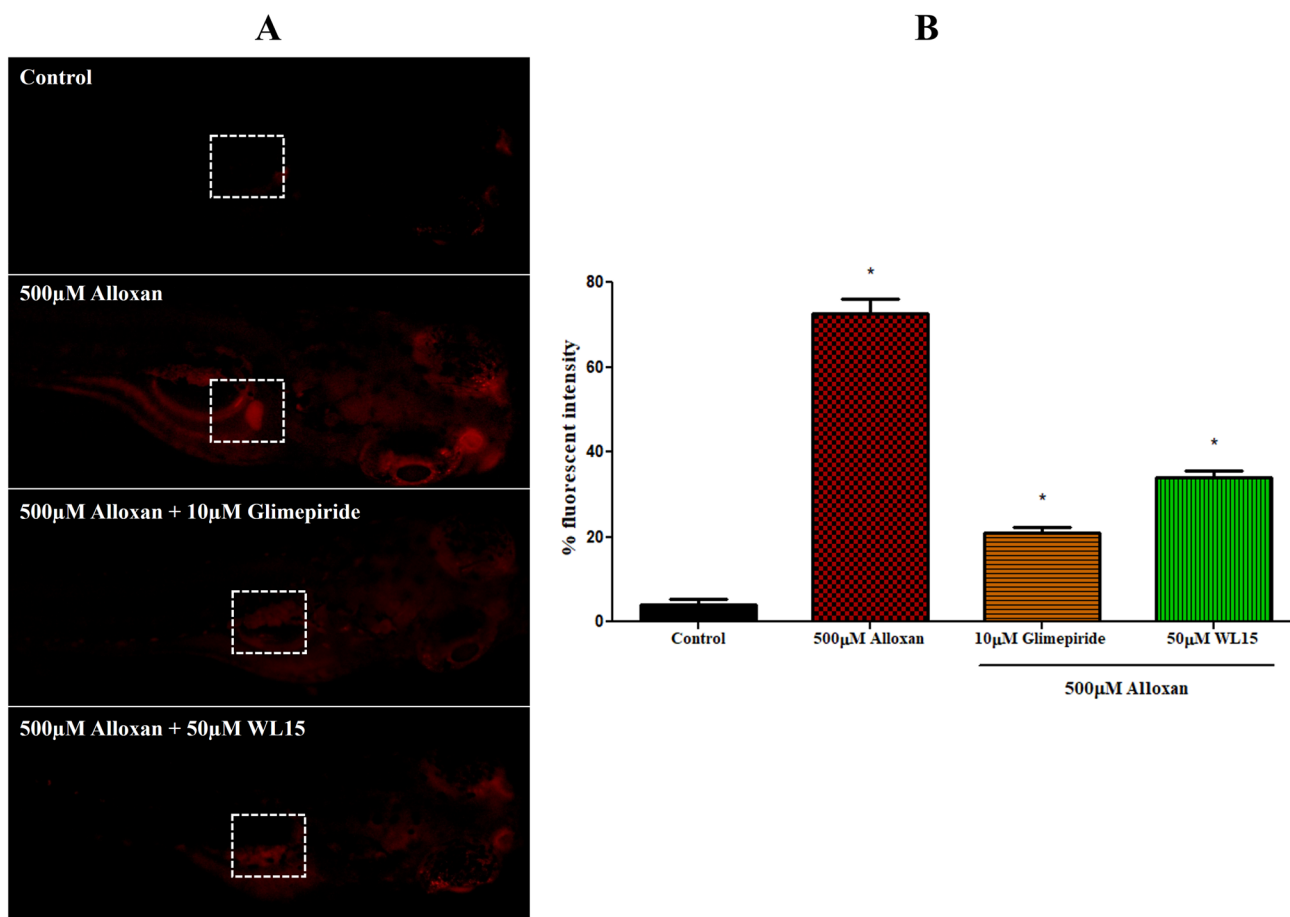


**Fig. 2** **A** Representative photomicrographs of apoptotic  $\beta$ -cells in zebrafish larvae ( $n=10/\text{group}$ ) stained by acridine orange fluorescent probe. **B** Quantitative analysis of *in-vivo* apoptosis in  $\beta$ -cells of zebrafish larvae. The fluorescence intensity was quantified using ImageJ. The untreated and glimepiride (10  $\mu\text{M}$ ) larvae were used

as control and positive control in the experiment, respectively. The  $\beta$ -cells are marked inside the white box. Experiments were performed in triplicate, and the data were expressed as mean  $\pm$  SD. \* represents the statistical significance at  $p < 0.05$

apoptosis (86%), and lipid peroxidation (73%) levels compared to untreated larvae (Figs. 1, 2, and 3). While the maximum decrease in ROS (30%), apoptosis (24%), and lipid peroxidation (34%) was observed in the 50  $\mu\text{M}$  of WL15 treatment group. These results showed that the WL15 peptide was protective against oxidative stress in  $\beta$ -cells of zebrafish larvae.

#### Effect of WL15 on superoxide anion and glutathione depletion.

The DHE and NDA staining were used to examine the effect of WL15 on reducing superoxide anion and glutathione depletion in  $\beta$ -cells of zebrafish larvae. In alloxan-exposed larvae, the fluorescent intensity of superoxide anion (77%) was higher, while a decrease in glutathione level (9%) was observed when compared to untreated larvae (Fig. 4 and 5). These superoxide anion levels (36%) in the  $\beta$ -cells of

zebrafish are reduced when WL15 peptides are cotreated with alloxan due to an increase in glutathione content (39%).

#### Effect of WL15 on alloxan induced $\beta$ -cells damages.

To investigate the protective effect of alloxan induced  $\beta$ -cells damages, the larvae were treated with 500  $\mu\text{M}$  of alloxan for 3 days. The alloxan exposed zebrafish larvae showed a decrease in fluorescent intensity, indicating a significant ( $p < 0.05$ ) decrease in the size of pancreatic  $\beta$ -cells in larvae (Fig. 6). However, cotreatment of WL15 (50  $\mu\text{M}$ ) increased the fluorescent intensity indicating the protective effect against  $\beta$ -cell damages and an increase in the size of  $\beta$ -cells in larvae.

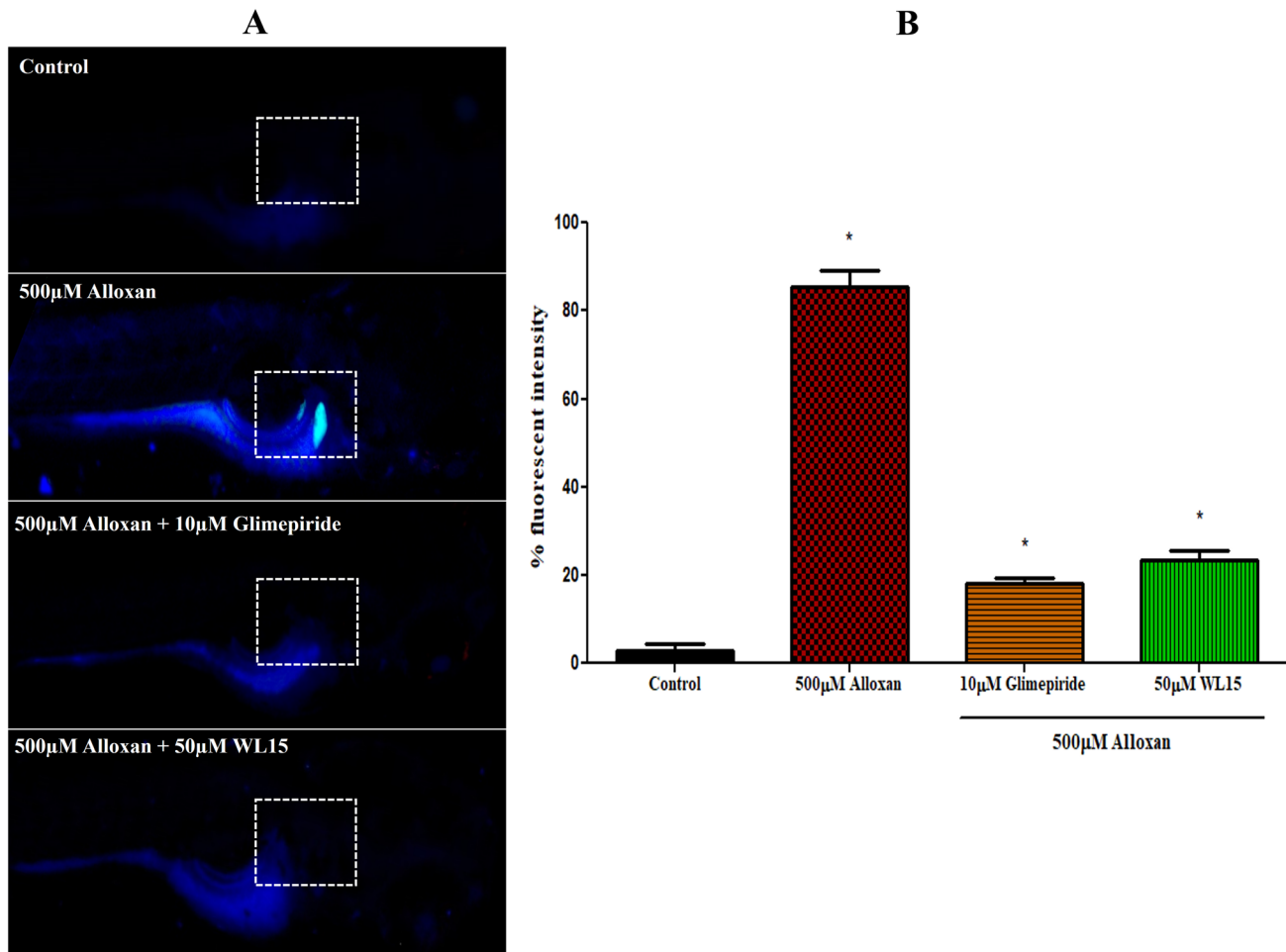


**Fig. 3** **A** Representative photomicrographs of lipid peroxidation in  $\beta$ -cells of zebrafish larvae ( $n = 10/\text{group}$ ) stained by DPPP fluorescent probe. **B** Quantitative analysis of *in-vivo* lipid peroxidation in  $\beta$ -cells of zebrafish larvae. The fluorescence intensity was quantified using ImageJ. The untreated and glimepiride (10  $\mu\text{M}$ ) larvae were used

as control and positive control in the experiment, respectively. The  $\beta$ -cells are marked inside the white box. Experiments were performed in triplicate, and the data were expressed as mean  $\pm$  SD. \* represents the statistical significance at  $p < 0.05$

### Glucose estimation.

The glucose levels were estimated in the zebrafish larvae using a glucose estimation kit. High glucose levels were observed in the 500  $\mu\text{M}$  alloxan treatment group (160 mg/dL) compared to the control group (84 mg/dL). A significant ( $p < 0.05$ ) reduction in the glucose level was observed in WL15 cotreated group (E-Suppl. Fig. 6). WL15 at 50  $\mu\text{M}$  was able to reverse the condition (113 mg/dL), similar to the glimepiride treatment (101 mg/dL). These results suggest that WL15 could attenuate post-prandial hyperglycemia conditions.

### Effect of WL15 on insulin and PEPCK expression.

The insulin expression in alloxan exposed larvae was investigated to check whether the WL15 can enhance the insulin

mRNA levels. The alloxan (500  $\mu\text{M}$ ) exposed larvae with  $\beta$ -cell damage showed a decrease in insulin expression level (0.35 fold), while when the WL15 peptide at 50  $\mu\text{M}$  was cotreated, the insulin level was significantly ( $p < 0.05$ ) upregulated (1.8 fold) (E-Suppl. Fig. 7A). Further the PEPCK expression was investigated, which transcriptionally regulated by insulin and act as a rate limiting step in gluconeogenesis. Overexpression of PEPCK causes excessive glucose production in the liver in patients with T2D. As a result inhibiting PEPCK has been proven to be a therapeutic target for lowering blood sugar. These findings prompted us to use real-time PCR to examine changes in PEPCK gene expression in response to WL15 treatment. When compared to the control group, alloxan increased PEPCK mRNA expression (2.2 fold) (E-Suppl. Fig. 7B). However, 50  $\mu\text{M}$  of WL15 cotreatment inhibited PEPCK mRNA expression (1.6 fold), respectively. This is comparable to the inhibitory

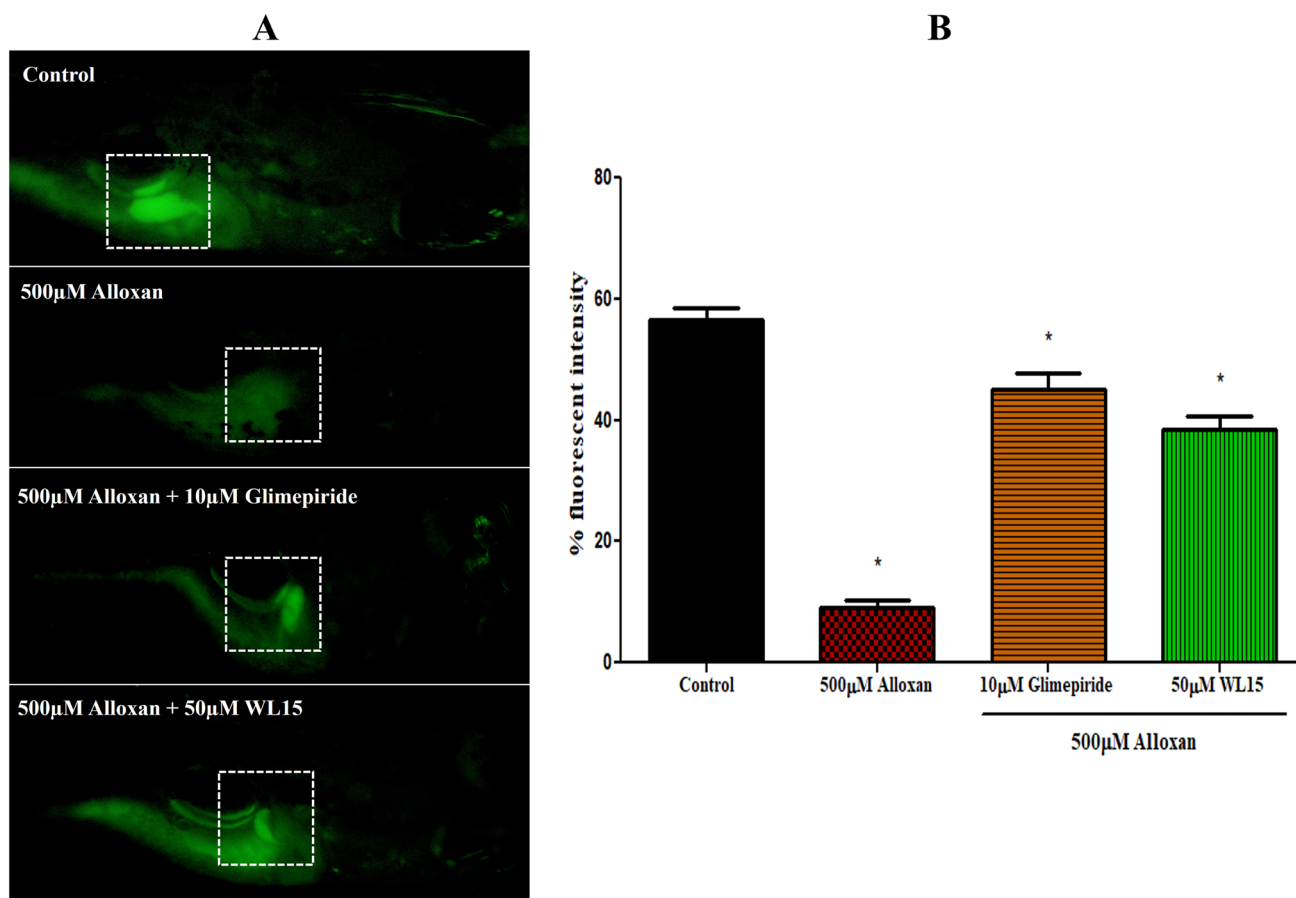


**Fig. 4** **A** Representative photomicrographs of glutathione level in  $\beta$ -cells of zebrafish larvae ( $n=10/\text{group}$ ) stained by NDA fluorescent probe. **B** Quantitative analysis of glutathione in  $\beta$ -cells of zebrafish larvae. The fluorescence intensity was quantified using ImageJ. The untreated and glimepiride ( $10\ \mu\text{M}$ ) larvae were used as control

and positive control in the experiment, respectively. The  $\beta$ -cells are marked inside the white box. Experiments were performed in triplicate, and the data were expressed as mean  $\pm$  SD. \* represents the statistical significance at  $p < 0.05$

efficacy of  $10\ \mu\text{M}$  of glimepiride on PEPCK expression (1.4 fold). From the result, we can assume that the inhibitory effect of WL15 on PEPCK expression is due to insulin upregulation. When taken together, WL15 may increase insulin production while decreasing PEPCK expression, resulting in normal glucose metabolism.

## Discussion

The teleost *C. striatus* had a higher amount of protein and essential amino acids, as determined by the proximate composition and amino acid content; when the right enzyme and protein are combined, a high yield of bioactive peptides is obtained [32]. In our previous studies [19, 20, 33, 34, 35], we reported that the proteins namely CSRP2, VPS26B, HATs, STPK, and CxxC in which the derived peptides including WL15, RF13, RW20, IW13, and MF18 possessed to have antioxidant, antidiabetic and antimicrobial properties. In

this observation, we initially screened these peptides for their better understanding of antioxidant and antidiabetic nature, especially on evaluating them on the  $\beta$ -cell damaged zebrafish *in-vivo* larval model. Using PeptideRanker and ToxinPred server, the toxicity and bioavailability of the peptides are investigated. All the five peptides of WL15, RF13, RW20, IW13, and MF18 are predicted to be non-toxic. While the WL15 peptide has better bioavailability compared to other peptides.

The antioxidant and antidiabetic activity of these peptides was predicted with molecular docking studies. The Protein Data Bank was used to obtain the protein structures of insulin receptors (PDB ID: 1IR3) and glutathione (PDB ID: 2I3Y). The peptides WL15, RF13, RW20, IW13, and MF18 are docked with insulin receptors and glutathione using HPEPDOCK webserver. In comparison to other peptides, WL15 had a higher affinity for binding to the insulin receptor and glutathione. Further, the *in-vitro* hydroxyl radical scavenging assay and  $\alpha$ -amylase assay were performed to



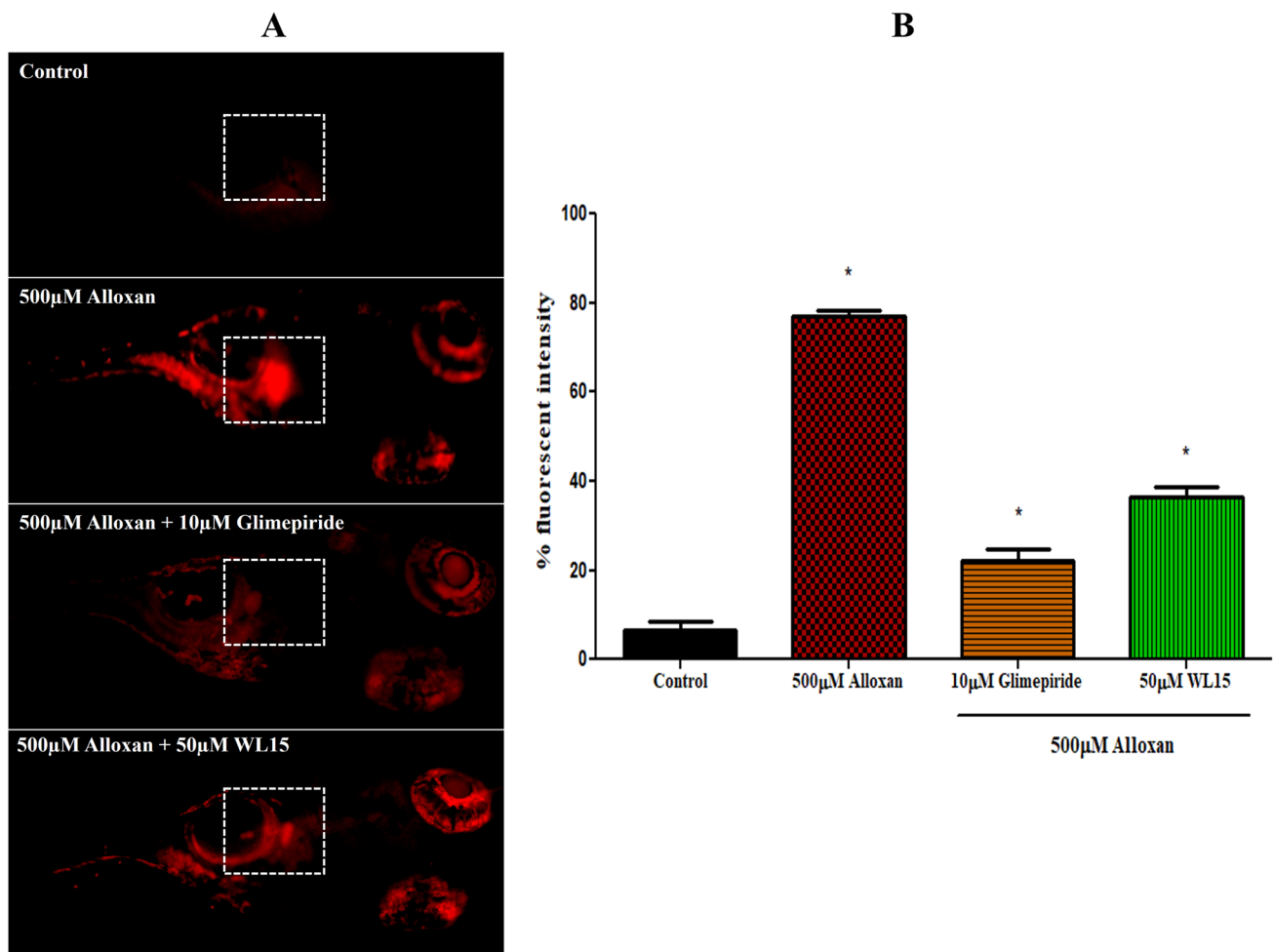


**Fig. 5** **A** Representative photomicrographs of superoxide anion in  $\beta$ -cells of zebrafish larvae ( $n=10/\text{group}$ ) stained by DHE fluorescent probe. **B** Quantitative analysis of superoxide anion in  $\beta$ -cells of zebrafish larvae. The fluorescence intensity was quantified using ImageJ. The untreated and glibenclamide ( $10 \mu\text{M}$ ) larvae were used

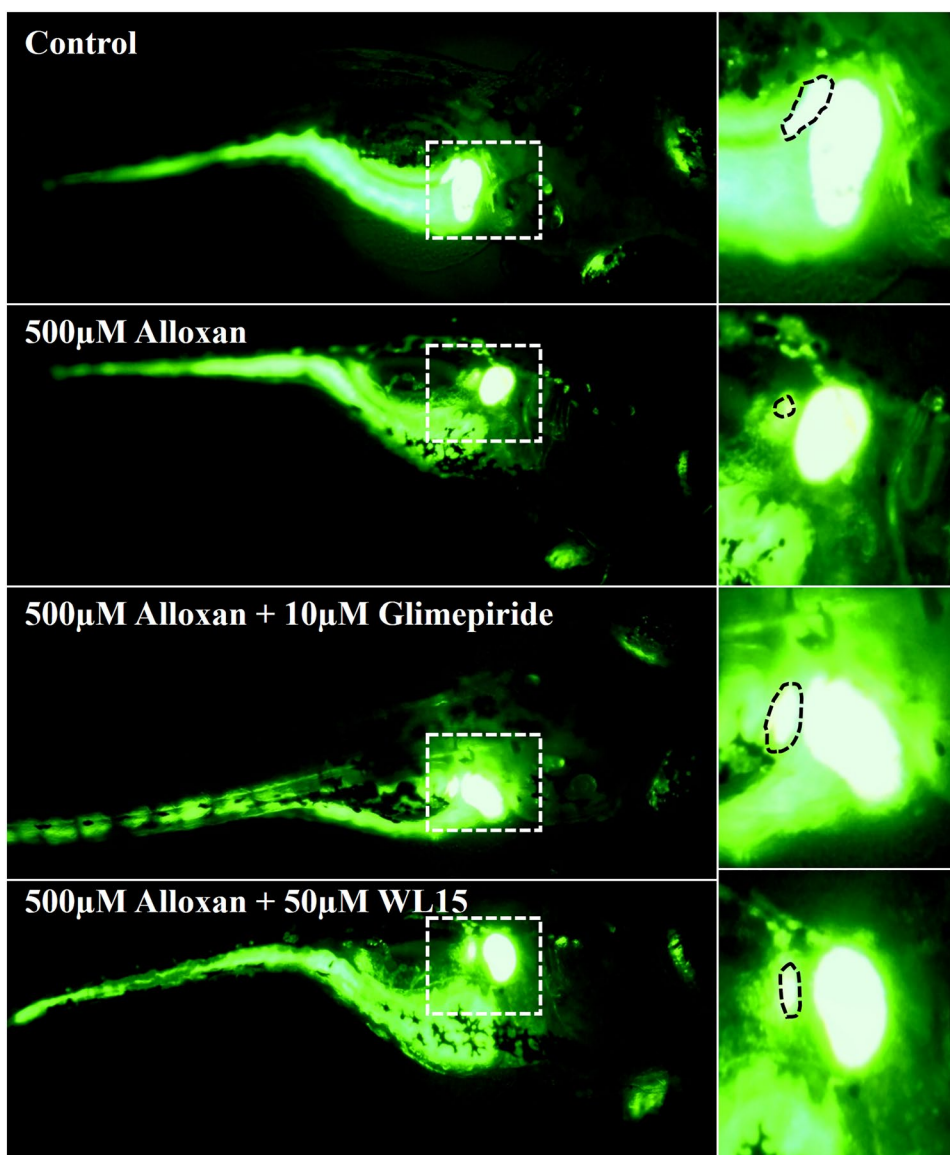
as control and positive control in the experiment, respectively. The  $\beta$ -cells are marked inside the white box. Experiments were performed in triplicate, and the data were expressed as mean  $\pm$  SD. \* represents the statistical significance at  $p < 0.05$

identify the peptides with better antioxidant and antidiabetic activity. The highly reactive species is the hydroxyl radical, which causes severe damage to nearby biomolecules. The presence of hydrogen donating ability in the compounds has a better ability to scavenge hydroxyl radicals [36]. On the other hand, if the  $\alpha$ -amylase enzyme is inhibited, starch is degraded into oligosaccharides and monosaccharides before being absorbed. As a result, glucose absorption is reduced, which lowers the post-prandial blood glucose levels [17]. In both hydroxyl radical scavenging and amylase inhibition assay, WL15 showed better activity compared to other peptides (RF13, RW20, IW13, and MF18). In addition, recent studies have identified antioxidant and antidiabetic properties of WL15 in both *in-vitro* and *in-vivo* models. The hydrophobic (leucine and alanine) and aromatic (phenylalanine and histidine) amino acids are present in the WL15 peptide,

which has strong antioxidant properties by transferring electrons to free radicals. Leucine and glycine are amino acids that are present in the WL15 peptide and have been shown to slow the progression of diabetes [10, 19]. However, no research has been conducted on the effect of WL15 peptide on normalizing glucose metabolism and reducing pancreatic toxicity, so the protective effect of WL15 peptide was investigated in the alloxan induced  $\beta$ -cell damaged zebrafish larvae model.

After being exposed to  $500 \mu\text{M}$  alloxan for 1 day, the oxidative stress in  $\beta$ -cells of zebrafish larvae was developed. Alloxan also reduces the survival and heartbeat rate of larvae with morphological abnormalities such as bent spine and bent tail. Mortality and heart rate have become sensitive indicators for evaluating the protective effect of WL15 due to these variations. The cotreatment of WL15 improved the

**Fig. 6** Effect of WL15 peptide on 2NBDG uptake in zebrafish larvae ( $n = 10/\text{group}$ ). The untreated and glimepiride ( $10 \mu\text{M}$ ) larvae were used as control and positive control in the experiment, respectively. The regeneration of  $\beta$ -cells of zebrafish larvae stained with 2NBDG is marked inside the white box



heartbeat rate and survival rate of  $500 \mu\text{M}$  alloxan exposed zebrafish larvae, while larvae are protected from abnormalities formation. Since WL15 at  $50 \mu\text{M}$  showed the highest activity range with no toxicity, this optimum concentration was taken for further experiments. Pancreatic cells are susceptible to oxidative stress due to their low antioxidant enzyme level of expression [37]. In diabetic animals, antioxidant defense systems in the  $\beta$ -cells are significantly disrupted in addition to increased free radical production [38]. Alloxan is specifically used for experimental diabetes conditions because it is selectively toxic to pancreatic  $\beta$ -cells and directly affects islet cell permeability by regulating ROS and lipid peroxidation production [39]. The amino acid composition of the WL15 are majorly leucine and glycine. By acting as a source of energy and regulating cell metabolism, leucine and glycine are known to encourage insulin release from

pancreatic  $\beta$ -cells. Additionally, leucine in peptides controls the expression of vital metabolic genes in  $\beta$ -cells to prevent islet dysfunction and diabetes [40]. According to the results (Figs. 5, 6), oxidative stress increased in the  $\beta$ -cells of the zebrafish larvae after exposure to alloxan. The WL15 at  $50 \mu\text{M}$  successfully reduced ROS and apoptosis, and the level of lipid peroxidation in the  $\beta$ -cells portion of the larvae was also significantly reduced. High levels of superoxide cause cellular dysfunction and apoptotic cell death, and they significantly increase in the organ during glutathione depletion [41]. Using DHE and NDA staining, it was discovered that alloxan significantly increased superoxide anion and depleted glutathione level in the  $\beta$ -cells region; however, the WL15 treatment group showed a gradual decrease in superoxide anion and normalized the glutathione level. It

indicates that the WL15 peptide inhibits ROS formation in the pancreatic  $\beta$ -cells.

Further, their effect on protecting the  $\beta$ -cells from damage and dysfunction was investigated in zebrafish larvae. To induce  $\beta$ -cells damages or dysfunction, the larvae are exposed to 500  $\mu$ M alloxan for 72 h. The 2NBDG treatment on zebrafish larvae allows for complete staining of  $\beta$ -cells [42]. In comparison to the control group, the size and fluorescent intensity of  $\beta$ -cells in the alloxan-exposed group decreased. The size of pancreatic beta cells was reduced due to damage, but damages were significantly ( $p < 0.05$ ) reduced, and pancreatic regeneration was observed after cotreatment with the WL15 peptide. Insulin is produced and released by  $\beta$ -cells in the pancreas in response to blood glucose levels.  $\beta$ -cells in people with T2D have to work harder to produce enough insulin to keep blood sugar levels under control. This condition may also lead to  $\beta$ -cell dysfunction [1]. WL15 peptide at 50  $\mu$ M was able to control the high glucose level equally compared to the positive control glimepiride (10  $\mu$ M) in the larvae. Some patients with T2D may experience hyperglycemia as a result of insulin inability to suppress the expression of PEPCK, a rate-limiting enzyme in gluconeogenesis. PEPCK overexpression has been previously reported to reduce insulin signaling and insulin sensitivity in transgenic mice [43]. In this study, the mRNA expression of insulin levels was downregulated, and PEPCK was upregulated in the alloxan-treated group, but this was reversed by the cotreatment of WL15, suggesting that WL15 may induce insulin secretion, thus reducing gluconeogenesis by blocking the expression of PEPCK.

In conclusion, we showed that WL15 could normalize glucose metabolism by selectively inhibiting PEPCK expression and increasing insulin levels. WL15 was also found to be protective against ROS-induced pancreatic toxicity. Thus, chronic WL15 peptide consumption may aid in treating hyperglycemia and preventing diabetic complications. The use of a larvae model limits this study and more research is needed to determine clinical relevance to humans.

**Supplementary Information** The online version contains supplementary material available at <https://doi.org/10.1007/s11033-022-07882-4>.

**Acknowledgements** The authors extend their sincere appreciation to the Researchers Supporting Project Number (RSP-2021/191), King Saud University, Riyadh, Saudi Arabia.

**Authors contribution** AG and JA contributed to the concept and design of the study; AG and GS performed the experiments; MHA, BOA, AJ and JA contributed significantly to resources, data analysis, manuscript preparation and perform the analysis with constructive discussions; JA supervised and checked the manuscript; All authors read and approved the final manuscript.

**Funding** Researchers Supporting Project Number (RSP-2021/191), King Saud University, Riyadh, Saudi Arabia.

**Data availability** The data used to support the findings of this study are available from the corresponding author upon request.

**Code availability** Not applicable.

## Declarations

**Conflict of interest** All authors declare that they have no conflict of interest.

**Ethical approval** This research does not involve any human objects; however, we have performed few assays using zebrafish embryo and larvae. The fish were handled and experimented carefully as per the Institute Animal Handling Procedure and Ethical Approval and Clearance (No. SAF/IAEC/211215/004).

**Consent to participate** All the authors listed in the manuscript have approved the manuscript.

**Consent for publication** The data provided in the manuscript is approved by all authors for publication.

## References

1. Cerf ME (2013) Beta cell dysfunction and insulin resistance. *Front Endocrinol (Lausanne)* 4:1–12. <https://doi.org/10.3389/fendo.2013.00037>
2. Saisho Y (2015)  $\beta$ -cell dysfunction: its critical role in prevention and management of type 2 diabetes. *World J Diabetes* 6:109. <https://doi.org/10.4239/wjd.v6.i1.109>
3. Gurgul-Convey E, Mehmeti I, Plötz T et al (2016) Sensitivity profile of the human EndoC- $\beta$ H1 beta cell line to proinflammatory cytokines. *Diabetologia* 59:2125–2133. <https://doi.org/10.1007/s00125-016-4060-y>
4. Drews G, Krippeit-Drews P, Duifer M (2010) Oxidative stress and beta-cell dysfunction. *Pflugers Arch Eur J Physiol* 460:703–718. <https://doi.org/10.1007/s00424-010-0862-9>
5. Eguchi N, Vaziri ND, Dafoe DC, Ichii H (2021) The role of oxidative stress in pancreatic  $\beta$  cell dysfunction in diabetes. *Int J Mol Sci* 22:1–18. <https://doi.org/10.3390/ijms22041509>
6. Stancill JS, Broniowska KA, Oleson BJ et al (2019) Pancreatic -cells detoxify H<sub>2</sub>O<sub>2</sub> through the peroxiredoxin/thioredoxin antioxidant system. *J Biol Chem* 294:4843–4853. <https://doi.org/10.1074/jbc.RA118.006219>
7. Matschinsky FM (1996) A lesson in metabolic regulation inspired by the glucokinase glucose sensor paradigm. *Diabetes* 45:223–241. <https://doi.org/10.2337/diab.45.2.223>
8. Moss LG, Caplan TV, Moss JB (2013) Imaging beta cell regeneration and interactions with islet vasculature in transparent adult zebrafish. *Zebrafish* 10:249–257. <https://doi.org/10.1089/zeb.2012.0813>
9. Zang L, Maddison LA, Chen W (2018) Zebrafish as a model for obesity and diabetes. *Front Cell Dev Biol* 6:1–13. <https://doi.org/10.3389/fcell.2018.00091>
10. Guru A, Issac PK, Saraswathi NT et al (2021) Deteriorating insulin resistance due to WL15 peptide from cysteine and glycine-rich protein 2 in high glucose-induced rat skeletal muscle L6 cells. *Cell Biol Int* 45:1698–1709. <https://doi.org/10.1002/cbin.11608>
11. Mohd Shafri MA, Abdul Manan MJ (2012) Therapeutic potential of the haruan (*Channa striatus*): from food to medicinal uses. *Malays J Nutr* 18:125–136

12. Wang J, Wang H (2017) Oxidative stress in pancreatic beta cell regeneration. *Oxid Med Cell Longev*. <https://doi.org/10.1155/2017/1930261>
13. Yu Z, Wu S, Zhao W et al (2018) Identification and the molecular mechanism of a novel myosin-derived ACE inhibitory peptide. *Food Funct* 9:364–370. <https://doi.org/10.1039/c7fo01558e>
14. Pearman NA, Ronander E, Smith AM, Morris GA (2020) The identification and characterisation of novel bioactive peptides derived from porcine liver. *Curr Res Food Sci* 3:314–321. <https://doi.org/10.1016/j.crfs.2020.11.002>
15. Cakir B, Okuyan B, Sener G, Tunali-Akbay T (2021) Investigation of beta-lactoglobulin derived bioactive peptides against SARS-CoV-2 (COVID-19): *in silico* analysis. *Eur J Pharmacol* 891:173781. <https://doi.org/10.1016/j.ejphar.2020.173781>
16. Velayutham M, Guru A, Gatasheh MK et al (2022) Molecular docking of SA11, RF13 and DI14 peptides from vacuolar protein sorting associated protein 26B against cancer proteins and *in vitro* investigation of its anticancer potency in Hep-2 cells. *Int J Pept Res Ther*. <https://doi.org/10.1007/s10989-022-10395-0>
17. Sangeetha R, Vedaasree N (2012) *In vitro*  $\alpha$ -amylase inhibitory activity of the leaves of thespesia populnea. *ISRN Pharmacol* 2012:1–4. <https://doi.org/10.5402/2012/515634>
18. Manjunathan T, Guru A, Arockiaraj J, Gopinath P (2021) 6-gingerol and semisynthetic 6-gingerdione counteract oxidative stress induced by ROS in zebrafish. *Chem Biodivers*. <https://doi.org/10.1002/cbdv.202100650>
19. Guru A, Lite C, Freddy AJ et al (2021) Intracellular ROS scavenging and antioxidant regulation of WL15 from cysteine and glycine-rich protein 2 demonstrated in zebrafish *in vivo* model. *Dev Comp Immunol* 114:103863. <https://doi.org/10.1016/j.dci.2020.103863>
20. Issac PK, Lite C, Guru A et al (2021) Tryptophan-tagged peptide from serine threonine-protein kinase of *Channa striatus* improves antioxidant defence in L6 myotubes and attenuates caspase 3–dependent apoptotic response in zebrafish larvae. *Fish Physiol Biochem* 47:293–311. <https://doi.org/10.1007/s10695-020-00912-7>
21. Sudhakaran G, Prathap P, Guru A et al (2022) Anti-inflammatory role demonstrated both *in vitro* and *in vivo* models using non-steroidal tetranortriterpenoid, Nimbin (N1) and its analogues (N2 and N3) that alleviate the domestication of alternative medicine. *Cell Biol Int* 24:327–332. <https://doi.org/10.1002/cbin.11769>
22. Velayutham M, Ojha B, Issac PK et al (2021) NV14 from serine O-acetyltransferase of cyanobacteria influences the antioxidant enzymes *in vitro* cells, gene expression against H2O2 and other responses *in vivo* zebrafish larval model. *Cell Biol Int* 45:2331–2346. <https://doi.org/10.1002/cbin.11680>
23. Sarkar P, Guru A, Raju SV et al (2021) GP13, an *Arthrospira* platensis cysteine desulfurase-derived peptide, suppresses oxidative stress and reduces apoptosis in human leucocytes and zebrafish (*Danio rerio*) embryo via attenuated caspase-3 expression. *J King Saud Univ - Sci* 33:101665. <https://doi.org/10.1016/j.jksus.2021.101665>
24. Sudhakaran G, Prathap P, Guru A et al (2022) Reverse pharmacology of Nimbin-N2 attenuates alcoholic liver injury and promotes the hepatoprotective dual role of improving lipid metabolism and downregulating the levels of inflammatory cytokines in zebrafish larval model. *Mol Cell Biochem*. <https://doi.org/10.1007/s11010-022-04448-7>
25. Haridevamuthu B, Manjunathan T, Guru A (2022) Amelioration of acrylamide induced neurotoxicity by benzo [ b ] thiophene analogs via glutathione redox dynamics in zebrafish larvae. *Brain Res* 1788:147941. <https://doi.org/10.1016/j.brainres.2022.147941>
26. Lite C, Guru A, Juliet MJ, Arockiaraj J (2022) Embryonic exposure to butylparaben and propylparaben induced developmental toxicity and triggered anxiety-like neurobehavioral response associated with oxidative stress and apoptosis in the head of zebrafish larvae. *Environ Toxicol*. <https://doi.org/10.1002/tox.23545>
27. Li Y, Li X, Chu Q et al (2020) *Russula alutacea* Fr. polysaccharide ameliorates inflammation in both RAW264.7 and zebrafish (*Danio rerio*) larvae. *Int J Biol Macromol* 145:740–749. <https://doi.org/10.1016/j.ijbiomac.2019.12.218>
28. Lee J, Jung DW, Kim WH et al (2013) Development of a highly visual, simple, and rapid test for the discovery of novel insulin mimetics in living vertebrates. *ACS Chem Biol* 8:1803–1814. <https://doi.org/10.1021/cb4000162>
29. Velayutham M, Guru A, Arasu MV et al (2021) GR15 peptide of *S-adenosylmethionine* synthase (SAME) from *Arthrospira platensis* demonstrated antioxidant mechanism against H2O2 induced oxidative stress in *in-vitro* MDCK cells and *in vivo* zebrafish larvae model. *J Biotechnol* 342:79–91. <https://doi.org/10.1016/j.jbiotec.2021.10.010>
30. Guru A, Sudhakaran G, Velayutham M et al (2022) Daidzein normalized gentamicin-induced nephrotoxicity and associated pro-inflammatory cytokines in MDCK and zebrafish: possible mechanism of nephroprotection. *Comp Biochem Physiol Part C Toxicol Pharmacol* 258:109364. <https://doi.org/10.1016/j.cbpc.2022.109364>
31. Haridevamuthu B, Manjunathan T, Guru A, Saravana R (2022) Hydroxyl containing benzo[b]thiophene analogs mitigates the acrylamide induced oxidative stress in the zebrafish larvae by stabilizing the glutathione redox cycle. *Life Sci*. <https://doi.org/10.1016/j.lfs.2022.120507>
32. Ghassem M, Arihara K, Babji AS et al (2011) Purification and identification of ACE inhibitory peptides from Haruan (*Channa striatus*) myofibrillar protein hydrolysate using HPLC-ESI-TOF MS/MS. *Food Chem* 129:1770–1777. <https://doi.org/10.1016/j.foodchem.2011.06.051>
33. Guru A, Velayutham M, Arockiaraj J (2022) Lipid-lowering and antioxidant activity of RF13 peptide from vacuolar protein sorting-associated protein 26B (VPS26B) by modulating lipid metabolism and oxidative stress in HFD induced obesity in zebrafish larvae. *Int J Pept Res Ther* 28:74. <https://doi.org/10.1007/s10989-022-10376-3>
34. Prabha N, Guru A, Harikrishnan R et al (2022) Neuroprotective and antioxidant capability of RW20 peptide from histone acetyltransferases caused by oxidative stress-induced neurotoxicity in *in vivo* zebrafish larval model. *J King Saud Univ - Sci* 100:101861. <https://doi.org/10.1016/j.jksus.2022.101861>
35. Nagaram P, Pasupuleti M, Arockiaraj J (2020) CxxC zinc finger protein derived peptide, MF18 functions against biofilm formation. *Protein J* 39:337–349. <https://doi.org/10.1007/s10930-020-09904-1>
36. Pavithra K, Vadivukkarasi S (2015) Evaluation of free radical scavenging activity of various extracts of leaves from *Kedrostis foetidissima* (Jacq.) Cogn. *Food Sci Hum Wellness* 4:42–46. <https://doi.org/10.1016/j.fshw.2015.02.001>
37. Lenzen S, Drinkgern J, Tiedge M (1996) Low antioxidant enzyme gene expression in pancreatic islets compared with various other mouse tissues. *Free Radic Biol Med* 20:463–466. [https://doi.org/10.1016/0891-5849\(96\)02051-5](https://doi.org/10.1016/0891-5849(96)02051-5)
38. Evans JL, Goldfine ID, Maddux BA, Grodsky GM (2002) Oxidative stress and stress-activated signaling pathways: a unifying hypothesis of type 2 diabetes. *Endocr Rev* 23:599–622. <https://doi.org/10.1210/er.2001-0039>
39. Ramkumar KM, Lee AS, Krishnamurthi K et al (2009) *Gymnema montanum* H. protects against alloxan-induced oxidative stress and apoptosis in pancreatic  $\beta$ -cells. *Cell Physiol Biochem* 24:429–440. <https://doi.org/10.1159/000257480>
40. Vahdatpour T, Nokhodchi A, Zakeri-Milani P et al (2019) Leucine–glycine and carnosine dipeptides prevent diabetes induced

- by multiple low-doses of streptozotocin in an experimental model of adult mice. *J Diabetes Investig* 10:1177–1188. <https://doi.org/10.1111/jdi.13018>
41. Moriya S, Yokoyama H, Fukuda M et al (2000) Glutathione depletion enhances the formation of superoxide anion released into hepatic sinusoids after lipopolysaccharide challenge. *Alcohol Clin Exp Res* 24:59–63. <https://doi.org/10.1111/j.1530-0277.2000.tb00014.x>
42. Nam YH, Hong BN, Rodriguez I et al (2015) Synergistic potentials of coffee on injured pancreatic islets and insulin action via KATP channel blocking in zebrafish. *J Agric Food Chem* 63:5612–5621. <https://doi.org/10.1021/acs.jafc.5b00027>
43. Kwon SJ, Hwang SJ, Jung Y et al (2017) A synthetic Nitraria alkaloid, isonitramine protects pancreatic  $\beta$ -cell and attenuates

post-prandial hyperglycemia. *Metabolism* 70:107–115. <https://doi.org/10.1016/j.metabol.2017.02.002>

**Publisher's Note** Springer Nature remains neutral with regard to jurisdictional claims in published maps and institutional affiliations.

Springer Nature or its licensor (e.g. a society or other partner) holds exclusive rights to this article under a publishing agreement with the author(s) or other rightsholder(s); author self-archiving of the accepted manuscript version of this article is solely governed by the terms of such publishing agreement and applicable law.

## Authors and Affiliations

Ajay Guru<sup>1</sup>  · Gokul Sudhakaran<sup>1</sup>  · Mikhlid H. Almutairi<sup>2</sup> · Bader O. Almutairi<sup>2</sup> · Annie Juliet<sup>3</sup> · Jesu Arockiaraj<sup>1</sup> 

Ajay Guru  
ajayrag02@gmail.com

Gokul Sudhakaran  
gokulsudhakaran98@gmail.com

Mikhlid H. Almutairi  
malmutari@ksu.edu.sa

Bader O. Almutairi  
bomotairi@ksu.edu.sa

Annie Juliet  
anniejuliet22@yahoo.com

<sup>1</sup> Department of Biotechnology, College of Science and Humanities, SRM Institute of Science and Technology, Kattankulathur 603 203, Chennai, Tamil Nadu, India

<sup>2</sup> Department of Zoology, College of Science, King Saud University, P.O. Box: 2455, Riyadh 11451, Saudi Arabia

<sup>3</sup> Foundation for Aquaculture Innovations and Technology Transfer (FAITT), Thoraipakkam, Chennai 600 097, Tamil Nadu, India